



Photopolymerization Hot Paper

How to cite: *Angew. Chem. Int. Ed.* **2021**, *60*, 10935–10941

International Edition: doi.org/10.1002/anie.202101322

German Edition: doi.org/10.1002/ange.202101322

# Wavelength-Selective Photopolymerization of Hybrid Acrylate-Oxetane Liquid Crystals

Davey C. Hoekstra, Bodine P. A. C. van der Lubbe, Tom Bus, Lanti Yang, Nadia Grossiord, Michael G. Debije, and Albert P. H. J. Schenning\*

**Abstract:** We report on the wavelength-selective photopolymerization of a hybrid acrylate-oxetane cholesteric liquid crystal monomer mixture. By controlling the sequence and rate of the orthogonal free-radical and cationic photopolymerization reactions, it is possible to control the degree of phase separation in the resulting liquid crystal interpenetrating networks. We show that this can be used to tune the reflective color of the structurally colored coatings produced. Conversely, the structural color can be used to monitor the degree of phase separation. Our new photopolymerization procedure allows for structuring liquid crystal networks in three dimensions, which has great potential for fabricating liquid crystal polymer materials with programmable functional properties.

## Introduction

Photopolymerization reactions are among the most widely used polymerization methods and allow for spatial control of the properties of the polymer materials.<sup>[1]</sup> Further control can be achieved by wavelength-selective or orthogonal photopolymerization reactions using different irradiation wavelengths.<sup>[2]</sup> Combined with the development of light emitting diode (LED) technology that provides greater precision over the irradiation wavelength,<sup>[3]</sup> these orthogonal photopolymerization processes have led to the advent of polymer materials that cannot be obtained through conven-

tional polymerization processes. Examples include the synthesis of well-defined topological polymers,<sup>[4–7]</sup> hierarchical structured materials,<sup>[8]</sup> multimaterial 3D printing,<sup>[9–11]</sup> and interpenetrating networks (IPNs) with programmed functional properties.<sup>[12,13]</sup>

Liquid crystal networks (LCNs) are an appealing class of advanced functional materials that are commonly produced via free-radical or cationic photopolymerization of liquid crystals that are functionalized with polymerizable groups.<sup>[14–18]</sup> For example in cholesteric liquid crystals, photopolymerization was used to precisely control the network formation by photolithography,<sup>[19–22]</sup> and photopolymerization-induced diffusion,<sup>[23]</sup> resulting in broad reflection bands,<sup>[24,25]</sup> super reflectivity,<sup>[26]</sup> and paintable LC displays.<sup>[27–29]</sup>

To date, the photopolymerization-induced diffusion of liquid crystals monomers has mostly been achieved by free-radical polymerization of mixtures of mono- and di-acrylate liquid crystals. Most liquid crystalline IPNs reported are in fact semi-IPNs that are prepared by swelling a polymer network with a second monomer that is subsequently polymerized,<sup>[30–33]</sup> or are partly prepared through thermal polymerization.<sup>[34]</sup> Hence, it would be appealing to develop liquid crystalline systems that can be polymerized through orthogonal polymerization reactions. This will allow for fabrication of IPNs and controlled phase separation in LC polymer materials with programmable properties.<sup>[35–38]</sup>

In this work, we report on the wavelength-selective photopolymerization of a hybrid acrylate-oxetane cholesteric liquid crystal mixture through orthogonal free-radical and cationic ring-opening polymerization reactions. A chiral dioxetane monomer was used to induce a cholesteric liquid crystalline phase and to create structural colors.<sup>[19]</sup> The resulting mixture was gravure coated and subsequently polymerized. Simultaneous polymerization of both the acrylate and oxetane LC monomers resulted in the formation of an interpenetrating LC network having a red structural color. A sequential approach, where the free-radical photopolymerization was performed first at a lower intensity led to photopolymerization-induced diffusion of the acrylate LC monomer, resulting in a phase-separated polyacrylate layer on top of the IPN structure and a blue structurally colored polymer. By monitoring structural color changes in the photonic polymer, we could follow the phase separation. The extent of phase separation could be engineered by varying the illumination time. Effectively, this allows for spatiotemporal control of not only where polymerization is initiated, but also control of the network structure through the

[\*] D. C. Hoekstra, B. P. A. C. van der Lubbe, T. Bus, Dr. M. G. Debije, Prof. A. P. H. J. Schenning  
Stimuli-responsive Functional Materials and Devices  
Department of Chemical Engineering and Chemistry  
Eindhoven University of Technology  
Groene Loper 3, 5612 AE, Eindhoven (The Netherlands)  
E-mail: a.p.h.j.schenning@tue.nl

D. C. Hoekstra, Prof. A. P. H. J. Schenning  
Institute for Complex Molecular Systems  
Eindhoven University of Technology  
Groene Loper 3, 5612 AE, Eindhoven (The Netherlands)

Dr. L. Yang, Dr. N. Grossiord  
T&I, SABIC  
Plasticslaan 1, 4612 PX, Bergen op Zoom (The Netherlands)

Supporting information and the ORCID identification number(s) for the author(s) of this article can be found under:  
<https://doi.org/10.1002/anie.202101322>.

© 2021 The Authors. *Angewandte Chemie International Edition* published by Wiley-VCH GmbH. This is an open access article under the terms of the Creative Commons Attribution Non-Commercial License, which permits use, distribution and reproduction in any medium, provided the original work is properly cited and is not used for commercial purposes.

film thickness. As a first application of this finding, we demonstrate the possibility of spatio-temporal control over the color of the cholesteric LC coatings to fabricate full-color patterned photonic polymers.

## Results and Discussion

The liquid crystal blend is comprised of liquid crystalline di-acrylate **1** and liquid crystalline di-oxetane **2** monomers (Figure 1 a). Both monomers exhibit a nematic LC phase. The addition of chiral oxetane monomer **3** results in a chiral-nematic LC phase in the blend, the reflective color of which can be tuned by the amount of **3** that is added.<sup>[19]</sup> The photoinitiator system consists of a free-radical initiator **4** and a photoacid generator **5** that is used to initiate the cationic ring-opening polymerization of the oxetane monomers. The absorption of free-radical initiator **4** is red-shifted, resulting in a non-overlapping region in the absorption spectra of **4** and **5** (Figure S1). This facilitates the wavelength-selective photopolymerization of both monomer species. Although the polymerization reactions themselves are orthogonal, the

initiator system is not entirely so. This means that the sequential photopolymerization must be carried out by first illuminating with blue light, resulting in the polymerization of the acrylate monomers. Subsequent illumination with UV light then polymerizes the oxetane monomers. The reverse order would result in the simultaneous polymerization of both monomer types, as illuminating with UV light results in activation of the free-radical initiator, and the photoacid generator has an intermediate step in which it also generates free radicals.

The monomer blends were dissolved in cyclopentanone to be coated by gravure printing. After printing the Ch-LC ink on a black PET substrate, evaporation of the solvent led to a cholesteric alignment that reflected red light. The monodomain alignment is induced by the biaxial orientation in the PET substrate. The coatings were then cured either simultaneously or sequentially. In the simultaneous approach, the entire spectrum (320–500 nm) was used to polymerize both monomer types at the same time. In the sequential approach, blue light was used first to polymerize the acrylate monomers. In the second step, UV light was used, to polymerize the oxetane monomers (Figure 1 b).

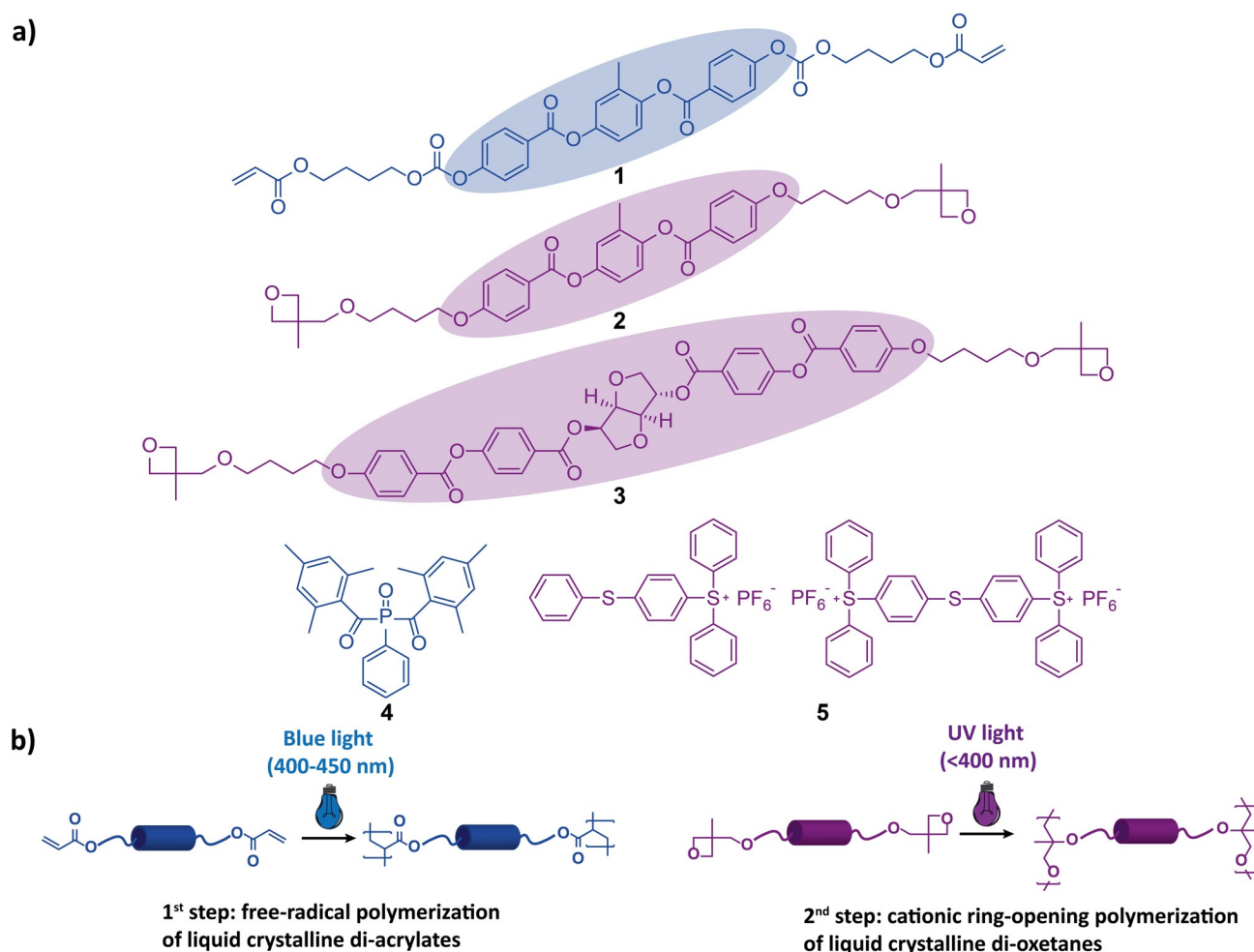


**Figure 1.** a) Monomer composition of the LC mixture used. b) Schematic representation of the two photopolymerization steps. In step 1, blue light is used, activating the radical initiator **4** resulting in the polymerization of the LC-diacrylates. In step 2, the use of UV light activates cationic initiator **5**, resulting in the polymerization of the LC di-oxetanes.

In the simultaneous polymerization procedure, 5 minutes of UV exposure at 55°C fixed the red-colored appearance of the photonic coating (Figure 2a). Atomic force microscopy (AFM) on a cross-section of the coating showed the presence of a cholesteric phase throughout the entire coating thickness (Figure 2b). The cholesteric pitch measured from this cross section was consistently homogeneous over the entire coating thickness and was measured to be approximately 397 nm. This pitch can be related to the central reflected wavelength via Equation (1)

$$\lambda_{\text{refl}} = n_{\text{av}} \times p \quad (1)$$

where  $p$  is the chiral nematic pitch. Assuming that  $n_{\text{av}} = 1.5$ ,<sup>[39]</sup> this results in  $\lambda_{\text{refl}} = 596$  nm, corresponding well with the reflection band measured with UV-VIS spectroscopy. Scanning electron microscopy (SEM) of the same cross-section revealed a similar result (Figure S2).

In the sequential procedure, however, when the first polymerization step was done for prolonged times (45 minutes) with a low intensity of blue light ( $0.1 \text{ mW cm}^{-2}$ ) at

55°C, a shift of the reflected color of the coating was observed. The originally red appearance of the coating had shifted to blue (Figure 2a). This shift already occurred during the first polymerization step; the second step, polymerization of the LC di-oxetane monomers, did not result in a further shift. The sequence of the polymerization reactions was monitored by FT-IR spectroscopy (Figure 2c). After coating of the Ch-LC monomer mixture, characteristic peaks corresponding to the acrylate groups ( $1410 \text{ cm}^{-1}$  and  $811 \text{ cm}^{-1}$ ) as well as the oxetane groups ( $975 \text{ cm}^{-1}$ ) were observed. The first illumination step (blue light) resulted in the disappearance of the peaks corresponding to the acrylate groups, whereas the oxetane peak at  $975 \text{ cm}^{-1}$  remained unchanged. After the second illumination step (UV light), this peak disappeared as well, indicating the conversion of the oxetane monomers. These results confirm that the wavelength-selective sequential polymerization of acrylate LC monomers followed by oxetane LC monomers is indeed possible.

AFM on cross-sections of the blue-shifted coating revealed the coating was divided in two regions (Figure 2d). On the bottom of the coating, from the interface with the PET

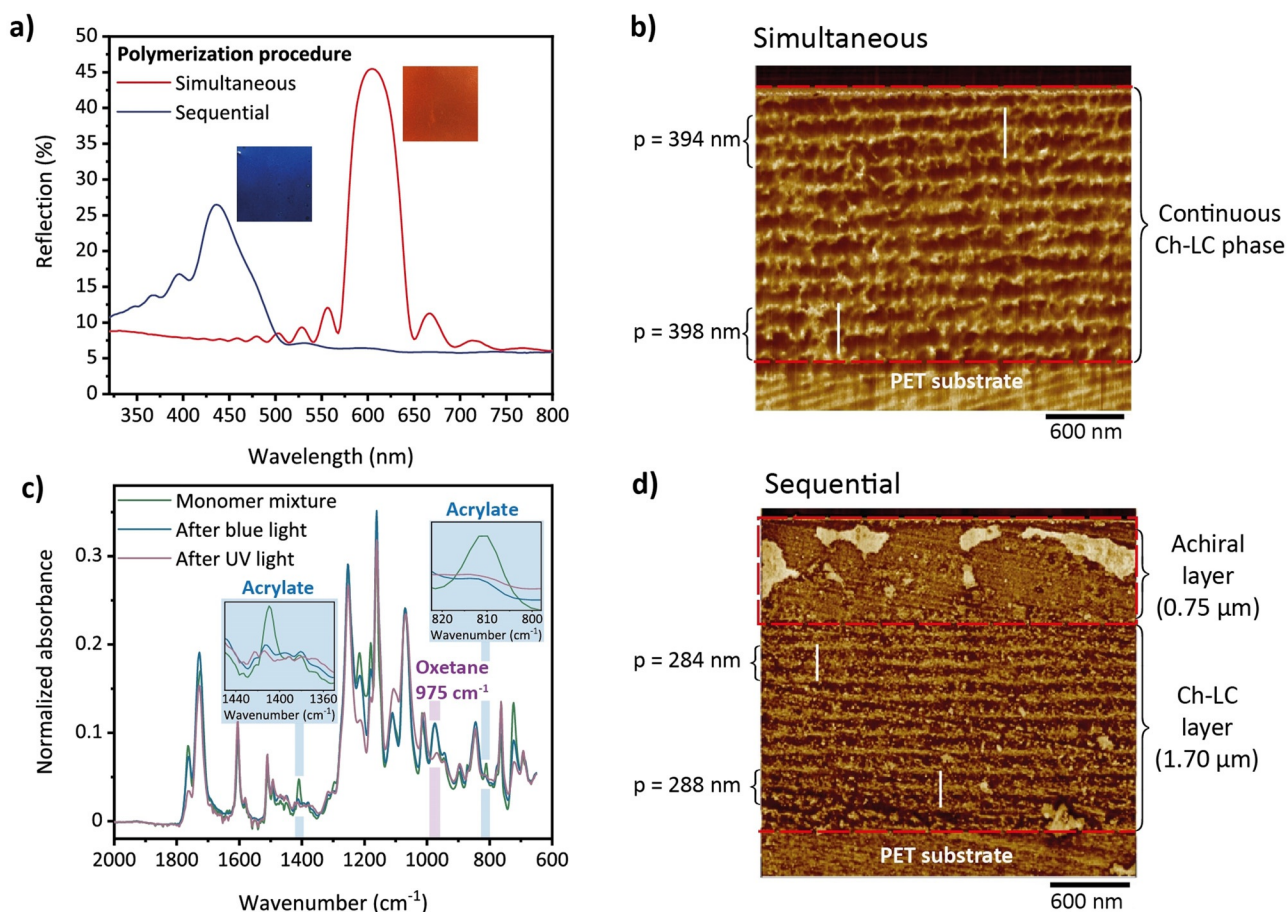


**Figure 2.** a) Reflection spectra of the Ch-LC coatings polymerized in the simultaneous (red line) and sequential (blue line) procedures. Photographs of the coatings are shown adjacent to the spectra. b) AFM analysis on a cross-section of the simultaneous photopolymerized coating. The sample displays a continuous cholesteric phase, with a constant pitch. c) FT-IR ATR analysis of the sequentially cured coating: the monomer mixture shows peaks corresponding to the acrylate groups (blue insets:  $1410 \text{ cm}^{-1}$  and  $811 \text{ cm}^{-1}$ ) and the oxetane groups ( $975 \text{ cm}^{-1}$ ). After the first polymerization step (blue light), only the acrylate peaks disappeared. After the second step (UV light), the oxetane peak disappeared as well. d) AFM analysis on a cross-section of a sequentially cured coating, with a 45 minute blue light illumination time. The coating has phase separated in a cholesteric layer with constant pitch throughout the entire layer thickness, and an achiral layer on top.

substrate, the periodic structure of a cholesteric phase can be clearly identified. The cholesteric pitch of this layer was measured to be 286 nm. On top of this cholesteric phase, a layer has emerged that does not show any periodicity. This implies that the chiral di-oxetane monomer **3** is either not present in this layer, or in a very low concentration. Effectively, this means that diffusion processes have taken place during the first polymerization step. During this step, only the liquid crystalline di-acrylate monomer is polymerizing. Given the low intensity of the blue light that is used, an intensity gradient through the coating thickness is likely to arise. Consequently, the di-acrylate LC monomers are depleting faster at the illuminated side of the coating, providing a driving force for diffusion of di-acrylate monomers towards the top of the coating. Based on the AFM analysis, we postulate that the di-oxetane LC and chiral monomers, that are not reactive in this step, counter diffuse towards the bottom of the coating. As a result, the polyacrylate layer on the top of the coating is most likely no longer chiral nematic. Concurrently, the concentration of chiral oxetane monomer **3** in the chiral nematic bottom layer has increased, which, according to Equation (2) explains the blue shift of the reflection band

$$\lambda_{\text{refl}} = \frac{n_{\text{av}}}{\text{HTP} \times [\text{C}]} \quad (2)$$

In this equation,  $\lambda_{\text{refl}}$  is the central reflected wavelength,  $n_{\text{av}}$  is the average refractive index of the LC monomers, HTP is the helical twisting power of chiral monomer **3** in the mixture and [C] is the concentration of **3**.

Remarkably, there is a clear interface between the chiral nematic and achiral layers. In previous works involving polymerization-induced diffusion in Ch-LC acrylate monomer blends, pitch-gradients were obtained, resulting in a broadened reflection band.<sup>[24,25]</sup> In this case, however, the reflection band is not obviously broadened. Moreover, image analysis of both AFM and SEM images of the cross section shows that the cholesteric pitch is constant throughout the cholesteric layer (Figure S3). According to Equation (1), the measured pitch (286 nm) should result in  $\lambda_{\text{refl}} = 429$  nm, corresponding well with the reflection band measured with UV-VIS spectroscopy. The clear transition between the Ch-LC and achiral layers, combined with no pitch-gradient forming in the sequentially polymerized coating can be explained by the infinite difference in reactivity between the two types of monomers in the first polymerization step, in which the oxetane monomers are not reacting at all. This allows for the sole diffusion of the acrylate monomers towards the top of the coating. We postulate that the helical twisting power of the chiral monomer is strong enough to maintain the chiral nematic phase until the acrylate monomers have diffused beyond its influence and become purely nematic. The coating then effectively becomes a bilayer of an achiral nematic layer consisting of an acrylate LCN and a cholesteric LC layer consisting of an interpenetrating network of oxetane LC monomers and acrylate LC monomers, albeit at lower concentrations.

To further confirm the sequential polymerization procedure is responsible for the induced phase separation, control experiments were conducted using a cholesteric LC mixture such consisting of only liquid crystalline acrylates or only liquid crystalline oxetanes: no color changes were observed upon sequential illumination with blue and UV light of the resulting coatings (Figure S4). Furthermore, leaving an unpolymerized coating in an oven at 55 °C for 24 hours did not result in a change in its reflection spectrum (Figure S5). These experiments indicate that the color change upon sequential free-radical and cationic photopolymerization must originate from the orthogonality of both mechanisms.

### Monitoring Polymerization-Induced Phase Separation by Structural Color Changes

We found that the extent of the induced blue-shift in the sequential photopolymerization process could be controlled by varying the blue light exposure time, with longer times resulting in a larger blue-shift of the reflection band. The reflection spectra show that after the coating procedure, the coating has a reflection band centered around 622 nm (Figure 3a). One minute of blue light illumination led to a reflection band that had the same central wavelength of reflection, yet with a reduced reflection and a narrower band. Longer blue light illumination times resulted in increasingly blue-shifted reflection bands. Alongside this blue shift, the reflection intensity decreased with longer illumination times. This could be ascribed to the combination of a relatively thin coating thickness, combined with the phase separation. The resulting cholesteric layers do not have sufficient thickness to accommodate the required number of cholesteric pitches to acquire the full 50% reflection limit of a cholesteric phase. At the same time, the rate of color change reduced upon longer free-radical polymerization, suggesting that the conversion of liquid crystalline diacrylate monomers results in sufficient vitrification in the system to retard the diffusion process responsible for the color change. Nevertheless, after 45 minutes of blue light illumination, it was possible to obtain a coating that reflected blue light (435 nm central reflection band). This means that the procedure presented is suitable to tune the reflection band of Ch-LC coatings over the entire visible spectrum using a single ink. The reflected color depends on the degree of phase separation. A higher degree of phase separation results in a thinner cholesteric layer with a higher concentration of chiral monomer **3**, and hence a blue-shift of the reflection band. No substantial additional color shift was observed for illumination times longer than 45 minutes.

Given that the change in appearance of the coatings is governed by the extent of photopolymerization-induced phase separation during sequential polymerization; this change in appearance can also be used to monitor the degree of phase separation. Using AFM analysis on cross-sections of the coatings, the degree of phase separation (defined as the ratio between the thickness of the phase separated achiral top layer and the total coating thickness) could be determined. This degree of phase of phase separation was plotted against

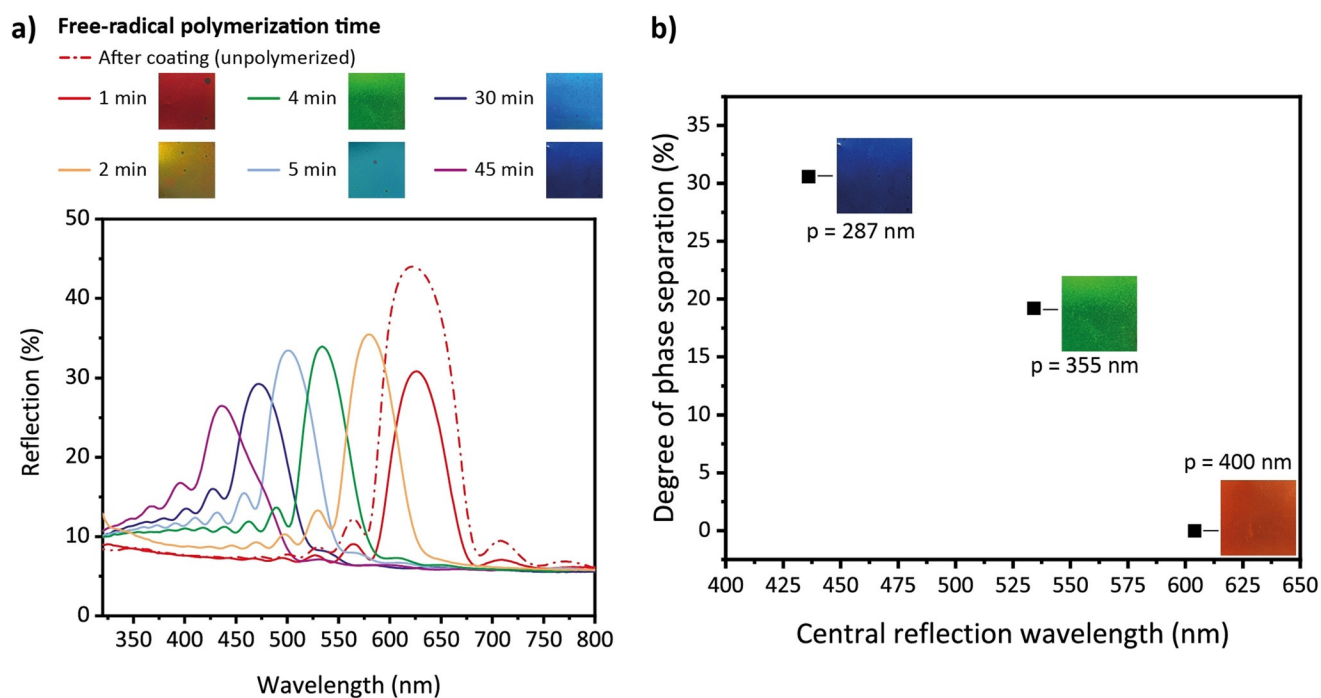


**Figure 3.** a) Reflection spectra of sequentially cured coatings in which the irradiation time of the first polymerization step is varied. Photographs of the corresponding coatings are shown in the legend. b) Degree of phase separation in the sequentially cured coatings (measured by AFM) as a function of the central reflection wavelength.

the measured central reflection wavelengths of the coatings (Figure 3b), revealing that with the current Ch-LC mixture, a red appearance amounts to little or no phase separation whereas, for instance, a blue appearance amounts to approximately 31 % phase separation. Therefore, the structural color can be used as an in situ analytical method to steer the amount of phase separation in the photonic polymer.

#### Patterned Full-Colored Photonic Polymers

As a direct application of the wavelength-selective polymerization procedure described above, patterned cholesteric coatings with multiple colors were prepared from a single Ch-LC ink. In a first approach, gravure-printed coatings that originally had a red reflection band were subjected to successive, masked blue light illumination (Figure 4a). First, the coating was illuminated with blue light ( $0.1 \text{ mWcm}^{-2}$ ) through the first mask for a relatively long time (45 minutes) to obtain a large blue shift (e.g. from red to blue). Subsequently, the coating was illuminated with blue light again through a second photomask for a shorter time, resulting in less blue shift in the pattern obtained (e.g. from red to green). Finally, a flood UV illumination was performed to freeze the red reflection from the areas that had not yet been illuminated, as well as to ensure maximum monomer conversion throughout the entire coating. With this approach, it is possible to obtain multicolored patterned coating with, for instance, 3 different colors (Figure 4b). The resolution of the produced patterns is good, mostly limited by the alignment of the consecutive photomasks, which must perfectly

align with the coating to achieve maximum resolution. No significant lateral diffusion was observed. Moreover, since the color of the coating is governed by the illumination time in the first polymerization step, a larger variety of colors would be possible by using more photomasks at different illumination times.

In a second approach, multicolor patterned coatings were obtained by using gradient greyscale masks in the first polymerization step (Figure 4c). With this approach, the color of the pattern obtained is determined by the intensity of blue light that is transmitted by the mask. Starting from a red-reflecting coating, areas of the mask with a high optical density allow for sufficient diffusion in the underlying coating to obtain a blue reflection band. In those areas of the coating that receive a higher intensity of blue light due to a lower optical density in the mask above, the extent of phase separation is limited due to vitrification caused by the increased conversion of acrylate monomers throughout the coating thickness. This results in limited blue shift of the initial red reflection. Furthermore, areas that are illuminated with the entire UV spectrum would not change their colored appearance. Hence, a multicolored pattern can be obtained using a single mask and a sequential polymerization procedure step with both blue light and UV light. The resulting pattern is shown in Figure 4d. The far-right region of the coating was photopolymerized at a high intensity ( $30 \text{ mWcm}^{-2}$ ) of both UV and blue light, which means it was effectively cured with the simultaneous polymerization approach, keeping its red structural color. The orange section remaining was also polymerized with UV and blue light, yet at a reduced intensity due to the greyscale mask. At this lower

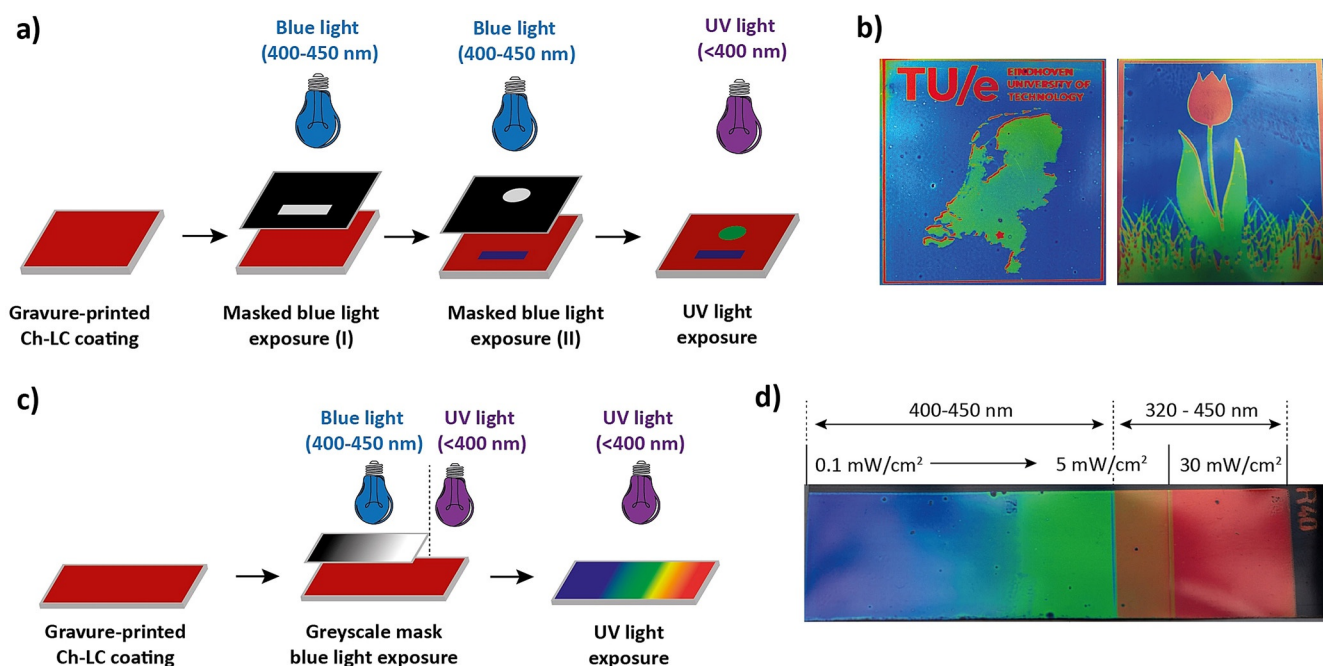


**Figure 4.** a) Preparation procedure for multicolor patterned Ch-LC coatings using multiple masks. b) Photographs of multicolor patterned Ch-LC coatings that were prepared using multiple masks at different illumination times. c) Preparation procedure for multicolor patterned Ch-LC coatings using grey scale masks. d) Photographs of multicolor patterned Ch-LC coatings that were prepared using greyscale masks.

intensity, the oxetane polymerization commences later than the acrylate polymerization (induction period),<sup>[40]</sup> allowing for limited phase separation that caused the reflection band to shift to orange. Finally, the left region was exposed to blue light with, due to the gradient greyscale mask, a gradient intensity, resulting in a gradient structural color from green to blue. This approach shows that the photopolymerization-induced phase separation can be controlled not only by varying the polymerization time, but also by varying the illumination spectrum as well as intensity in the first polymerization step.

## Conclusion

The wavelength-selective photopolymerization of a hybrid acrylate-oxetane liquid crystal mixture is reported, leading to LC polymer materials that cannot be obtained through conventional single polymerization processes. The LC monomers in the coatings polymerize through orthogonal polymerization mechanisms that can either be performed simultaneously, or sequentially. In case of simultaneous polymerization, a cholesteric interpenetrating network is obtained, while in the sequential polymerization procedure, photopolymerization-induced diffusion occurs, resulting in the formation of a bilayer of a cholesteric interpenetrating network and an achiral polyacrylate layer in the coating. Since the relative volumes of these layers determine the pitch of a chiral nematic phase, it is possible to control the color of the coating by varying the polymerization time, or the intensity of the illumination source. Conversely, the structural color of the coating can be used as an in situ analytical method

to monitor phase separation and allows for detailed control over the degree of phase separation throughout the thickness of the polymer.

The presented wavelength-selective photopolymerization process of hybrid acrylate-oxetane liquid crystals is vital for liquid crystal polymer materials with programmable functional properties. In this liquid crystal mixture, the network structure can be controlled to fabricate polymers ranging from LC IPNs to phase separated LCNs. With the addition of patterned photomasks, LCNs can even be structured in three dimensions. Towards future applications, the process could be further simplified by using a projector that is able to emit UV and blue light at different intensities.

## Acknowledgements

The authors would like to thank Sterre Bakker and Dr. Ellen van Heeswijk for initial experiments, and Prof. Dirk Broer and Dr. Johan Lub for valuable discussions. This work was financially supported by the Netherlands Organization for Scientific Research (TOP-PUNT 718.016.003).

## Conflict of interest

The authors declare no conflict of interest.

**Keywords:** cholesteric liquid crystals · in situ characterization · interpenetrating polymer networks · phase separation · photopolymerization

- [1] N. Corrigan, J. Yeow, P. Judzewitsch, J. Xu, C. Boyer, *Angew. Chem. Int. Ed.* **2019**, *58*, 5170–5189; *Angew. Chem.* **2019**, *131*, 5224–5243.
- [2] N. Corrigan, M. Ciftci, K. Jung, C. Boyer, *Angew. Chem. Int. Ed.* **2021**, *60*, 1748–1781; *Angew. Chem.* **2021**, *133*, 1774–1809.
- [3] C. Dietlin, S. Schweizer, P. Xiao, J. Zhang, F. Morlet-Savary, B. Graff, J. P. Fouassier, J. Lalevée, *Polym. Chem.* **2015**, *6*, 3895–3912.
- [4] K. Hildebrandt, M. Kaupp, E. Molle, J. P. Menzel, J. P. Blinco, C. Barner-Kowollik, *Chem. Commun.* **2016**, *52*, 9426–9429.
- [5] J. Xu, S. Shanmugam, C. Fu, K. F. Aguey-Zinsou, C. Boyer, *J. Am. Chem. Soc.* **2016**, *138*, 3094–3106.
- [6] S. Shanmugam, J. Cuthbert, T. Kowalewski, C. Boyer, K. Matyjaszewski, *Macromolecules* **2018**, *51*, 7776–7784.
- [7] B. M. Peterson, V. Kottisch, M. J. Supej, B. P. Fors, *ACS Cent. Sci.* **2018**, *4*, 1228–1234.
- [8] S. Xu, J. Yeow, C. Boyer, *ACS Macro Lett.* **2018**, *7*, 1376–1382.
- [9] N. D. Dolinski, Z. A. Page, E. B. Callaway, F. Eisenreich, R. V. Garcia, R. Chavez, D. P. Bothman, S. Hecht, F. W. Zok, C. J. Hawker, *Adv. Mater.* **2018**, *30*, 1800364.
- [10] S. Bialas, L. Michalek, D. E. Marschner, T. Krappitz, M. Wegener, J. Blinco, E. Blasco, H. Frisch, C. Barner-Kowollik, *Adv. Mater.* **2019**, *31*, 1807288.
- [11] Y. Y. Xu, Z. F. Ding, F. Y. Liu, K. Sun, C. Dietlin, J. Lalevée, P. Xiao, *ACS Appl. Mater. Interfaces* **2020**, *12*, 1658–1664.
- [12] X. Zhang, W. Xi, S. Huang, K. Long, C. N. Bowman, *Macromolecules* **2017**, *50*, 5652–5660.
- [13] L. Michalek, S. Bialas, S. L. Walden, F. R. Bloesser, H. Frisch, C. Barner-Kowollik, *Adv. Funct. Mater.* **2020**, *30*, 2005328.
- [14] J. Lub, D. J. Broer, R. A. Hikmet, K. G. Nierop, *Liq. Cryst.* **1995**, *18*, 319–326.
- [15] H. K. Bisoyi, Q. Li, *Chem. Rev.* **2016**, *116*, 15089–15166.
- [16] D. Y. Kim, K. M. Lee, T. J. White, K. U. Jeong, *NPG Asia Mater.* **2018**, *10*, 1061–1068.
- [17] A. J. J. Kragt, D. J. Broer, A. P. H. J. Schenning, *Adv. Funct. Mater.* **2018**, *28*, 1704756.
- [18] O. M. Wani, A. P. H. J. Schenning, A. Priimagi, *J. Mater. Chem. C* **2020**, *8*, 10191–10196.
- [19] D. C. Hoekstra, K. Nickmans, J. Lub, M. G. Debije, A. P. H. J. Schenning, *ACS Appl. Mater. Interfaces* **2019**, *11*, 7423–7430.
- [20] E. P. A. van Heeswijk, L. Yang, N. Grossiord, A. P. H. J. Schenning, *Adv. Funct. Mater.* **2020**, *30*, 1906833.
- [21] P. Zhang, X. Shi, A. P. H. J. Schenning, G. Zhou, L. T. de Haan, *Adv. Mater. Interfaces* **2020**, *7*, 1901878.
- [22] Q. Mo, B. Liu, W. Huang, P. Z. Sun, Z. Li, H. K. Bisoyi, D. Shen, Z. G. Zheng, Y. Q. Lu, Q. Li, *Adv. Opt. Mater.* **2020**, *8*, 2000155.
- [23] D. J. Broer, G. N. Mol, J. A. M. M. van Haaren, J. Lub, *Adv. Mater.* **1999**, *11*, 573–578.
- [24] D. J. Broer, J. Lub, G. N. Mol, *Nature* **1995**, *378*, 467–469.
- [25] E. P. A. van Heeswijk, J. J. H. Kloos, J. De Heer, T. Hoeks, N. Grossiord, A. P. H. J. Schenning, *ACS Appl. Mater. Interfaces* **2018**, *10*, 30008–30013.
- [26] A. J. J. Kragt, D. C. Hoekstra, S. Stallinga, D. J. Broer, A. P. H. J. Schenning, *Adv. Mater.* **2019**, *31*, 1903120.
- [27] R. Penterman, S. I. Klink, H. De Koning, G. Nisato, *Nature* **2002**, *417*, 55–58.
- [28] A. Ranjkesh, T. H. Yoon, *ACS Appl. Mater. Interfaces* **2019**, *11*, 26314–26322.
- [29] H. Khandelwal, E. P. A. van Heeswijk, A. P. H. J. Schenning, M. G. Debije, *J. Mater. Chem. C* **2019**, *7*, 7395–7398.
- [30] Y. Zhao, G. Yuan, *Macromolecules* **1996**, *29*, 1067–1069.
- [31] J. E. Stumpel, E. R. Gil, A. B. Spoelstra, C. W. M. Bastiaansen, D. J. Broer, A. P. H. J. Schenning, *Adv. Funct. Mater.* **2015**, *25*, 3314–3320.
- [32] T. Ube, K. Minagawa, T. Ikeda, *Soft Matter* **2017**, *13*, 5820–5823.
- [33] K. G. Noh, S. Y. Park, *Adv. Funct. Mater.* **2018**, *28*, 1707562.
- [34] H. F. Lu, M. Wang, X. M. Chen, B. P. Lin, H. Yang, *J. Am. Chem. Soc.* **2019**, *141*, 14364–14369.
- [35] L. Zhang, K. Li, W. Hu, H. Cao, Z. Cheng, W. He, J. Xiao, H. Yang, *Liq. Cryst.* **2011**, *38*, 673–677.
- [36] L. Xiao, H. Cao, J. Sun, H. Wang, D. Wang, Z. Yang, W. He, J. Xiao, H. Ding, H. Yang, *Liq. Cryst.* **2016**, *43*, 1299–1306.
- [37] M. Y. Duan, H. Cao, Y. Wu, E. L. Li, H. H. Wang, D. Wang, Z. Yang, W. L. He, H. Yang, *Phys. Chem. Chem. Phys.* **2017**, *19*, 2353–2358.
- [38] D. Zhang, H. Cao, M. Duan, H. Wang, Y. Chen, C. Zong, P. Gan, L. Zhao, Z. Yang, D. Wang, W. He, *J. Polym. Sci. Part B* **2019**, *57*, 1126–1132.
- [39] R. A. M. Hikmet, J. Lub, P. Maassen vd Brink, *Macromolecules* **1992**, *25*, 4194–4199.
- [40] U. Bulut, J. V. Crivello, *J. Polym. Sci. Part A* **2005**, *43*, 3205–3220.

Manuscript received: January 27, 2021

Revised manuscript received: February 4, 2021

Accepted manuscript online: February 23, 2021

Version of record online: March 26, 2021